Biochemical and Biophysical Research Communications 469 (2016) 587–592

Contents lists available at ScienceDirect

Biochemical and Biophysical Research Communications

journal homepage: www.elsevier.com/locate/ybbrc

The modeling of Alzheimer's disease by the overexpression of mutant Presenilin 1 in human embryonic stem cells

Makoto Honda [a, 1], Itsunari Minami [b], Norie Tooi [b], Nobuhiro Morone [b], Hisae Nishioka [b], Kengo Uemura [c], Ayae Kinoshita [d], John E. Heuser [b, e], Norio Nakatsuji [b, f], Kazuhiro Aiba [a, b, *]

[a] Stem Cell and Drug Discovery Institute, Kyoto 600-8813, Japan
[b] Institute for Integrated Cell-Material Sciences (WPI-iCeMS), Kyoto University, Kyoto 606-8501, Japan
[c] Department of Neurology, Kyoto University Graduate School of Medicine, Kyoto 606-8507, Japan
[d] School of Human Health Sciences, Kyoto University Graduate School of Medicine, Kyoto 606-8507, Japan
[e] Department of Cell Biology, Washington University, St. Louis, MO 63110, USA
[f] Institute for Frontier Medical Sciences, Kyoto University, Kyoto 606-8507, Japan

ARTICLE INFO

Article history:
Received 23 November 2015
Accepted 4 December 2015
Available online 10 December 2015

Keywords:
Human embryonic stem cell
Alzheimer's disease
Cellular disease model
Presenilin 1
Synaptic dysfunction

ABSTRACT

Cellular disease models are useful tools for Alzheimer's disease (AD) research. Pluripotent stem cells, including human embryonic stem cells (hESCs) and induced pluripotent stem cells (iPSCs), are promising materials for creating cellular models of such diseases. In the present study, we established cellular models of AD in hESCs that overexpressed the mutant Presenilin 1 (PS1) gene with the use of a site-specific gene integration system. The overexpression of PS1 did not affect the undifferentiated status or the neural differentiation ability of the hESCs. We found increases in the ratios of amyloid-β 42 (Aβ42)/Aβ40 and Aβ43/Aβ40. Furthermore, synaptic dysfunction was observed in a cellular model of AD that overexpressed mutant PS1. These results suggest that the AD phenotypes, in particular, the electrophysiological abnormality of the synapses in our AD models might be useful for AD research and drug discovery.

1. Introduction

Alzheimer's disease (AD) is one of the most common types of progressive dementia in the elderly population. It is characterized by some key features, including the deposition of amyloid beta (Aβ) peptide plaques, the formation of neurofibrillary tangles and the loss of neurons [1,2]. According to the amyloid cascade hypothesis, the extracellular accumulation of Aβ peptides acts as a trigger for the onset of AD; this is followed by changes in the presynaptic proteins and the loss of synapses in the AD patient's brain [3–5]. Cognitive ability is thought to be dependent on the synapse function of the neurons [6].

AD is classified into sporadic and familial types [7]. Presenilin 1 (PS1) is one of the genes responsible for familial AD [7,8]. PS1 is a catalytic core of γ-secretase and is produced from amyloid precursor protein by Aβ species such as Aβ40, Aβ42 and Aβ43 [9,10]. Mutant PS1 transgenic mice show some of the phenotypes of AD, including an increased level of Aβ42 and age-related neuronal loss [11,12].

In spite of the huge efforts of researchers, there are currently no fundamental therapeutic agents for AD. At present, pluripotent stem cells (PSCs) such as human embryonic stem cells (hESCs) and induced pluripotent stem cells (hiPSCs) are becoming promising materials for basic research and cell-based therapies. PSCs are self-renewing cells which have the ability to differentiate into any type of cell in the human body. This ability has led to hPSC-derived cellular disease models which can be an unlimited source for numerous types of cells for disease research and pharmacological studies [13–15].

Abbreviations: hPSC, human pluripotent stem cell; hESC, human embryonic stem cell; hiPSC, human induced pluripotent stem cell; AD, Alzheimer's disease; PS1, presenilin 1; Aβ, amyloid beta; ALS, amyotrophic lateral sclerosis; SOD1, superoxide dismutase 1; HPRT1, hypoxanthine phosphoribosyltransferase 1.

* Corresponding author. Institute for Integrated Cell-Material Sciences (WPI-iCeMS), Kyoto University Yoshida-Ushinomiyacho, Sakyo-ku, Kyoto 606-8501, Japan.
E-mail address: kaiba@icems.kyoto-u.ac.jp (K. Aiba).
[1] Current address. ReproCELL Inc., Yokohama, Kanagawa 222-0033, Japan.

http://dx.doi.org/10.1016/j.bbrc.2015.12.025

One of methods generating cellular AD models is the use of iPSC technology. Several studies have reported the establishment of various AD patient-specific iPSC lines and AD phenotypes, in models of AD (reviewed in Ref. [16]). However, models which replicate the electrophysiological abnormalities of synapses have not yet been reported. Moreover, it is difficult to accurately compare patient-specific iPSCs with healthy cells because of their different genomic backgrounds. Isogenic iPSC lines can be generated with the use of genome-editing methods [17,18]. However, the creation of multiple isogenic iPSC lines with this technology is time-consuming and not cost-effective.

Recently, we developed a site-directed gene integration system [19]. Using this system, we have already established hESC lines which overexpress superoxide dismutase 1 (SOD1), a gene which is responsible for amyotrophic lateral sclerosis (ALS), and showed that our ALS models, which had different mutations, displayed different drug responses [20]. In this study, we established hESC lines which overexpressed mutant PS1 using the site-directed gene integration system to create cellular models of AD. We found that our AD models showed AD phonotypes, including synaptic dysfunction.

2. Material and methods

2.1. The culture of hESCs

The procedure for maintaining the KhES-1 and KhES-1-HS hESC lines was essentially the same as that which was previously described [19,21]. The use of the hESC lines conformed to the Guidelines for Derivation and Utilization of Human Embryonic Stem Cells of the Ministry of Education, Culture, Sports, Science, and Technology of Japan.

2.2. The establishment of hESC lines which overexpressed mutant PS1 by the site-specific gene integration method

To establish hESC lines that overexpressed the PS1 gene, we utilized the KhES-1-HS hESC line, which was the parent cell line for the hypoxanthine phosphoribosyltransferase 1 (*HPRT1*) locus specific-gene integration system [19]. The expression vectors for wild-type and mutant PS1 cDNA (P117L, G378E, and D385A) were constructed. The resulting PS1 expression vectors were introduced into KhES-1-HS along with pEF1-Cre, as described in the previous paper [19]. Karyotype analyses of the PS1-overexpressing clones were carried out by Chromosome Science Lab, Inc. (Japan).

2.3. The neural differentiation of hESCs

Undifferentiated hESCs were cultured in N2B27 neural induction medium supplemented with both 100 ng/ml recombinant mouse noggin (R&D systems) or 100 nM LDN193189 (Cellagen Technology), and 1 μM SB431542 (Sigma–Aldrich) on poly-L-lysine (PLL)/Laminin111 (LM)-coated culture dishes. After 7–10 days, the cell colonies were dissociated into cell clumps using collagenase (GIBCO) and cultured in N2B27 medium with noggin or LDN193189 alone for the following 7–10 days. The cell colonies were enzymatically dissociated into cell clumps again and cultured in N2B27 induction medium. After 5–6 days, the cells were dissociated into single cells by Accutase (Innovative Cell Technologies), and cultured in N2B27 supplemented with 10 ng/ml of brain-derived neurotrophic factor, 10 ng/ml of neurotrophin-3 and 100 ng/ml of nerve growth factor (all from NGF, R&D Systems) on PLL, LM and fibronectin-coated dishes for neural maturation. After 7 days, the cells were treated with 1 μM Cytosine β-D-arabinofuranoside (Sigma–Aldrich).

2.4. Immunocytochemistry

The cells were fixed in freshly prepared 4% paraformaldehyde and permeabilized by 0.5% Triton-X (Wako Chemicals, Japan). The primary antibodies used in this study included polyclonal antibodies against NANOG (ReproCELL), βIII-tubulin (Abcam), or monoclonal antibodies against OCT3/4 (Santa Cruz Biotechnology), NeuN (Chemicon), SSEA4 (Chemicon), TRA1-60 (Chemicon). Alexa Fluor 488 and 568 goat anti-mouse immunoglobulin G, Alexa Fluor 488 goat anti-mouse immunoglobulin M, and Alexa Fluor 488 and 568 goat anti-rabbit IgG (Molecular Probes) were used as secondary antibodies. The cells were counterstained with 4,6-diamidino-2-phenylindole (DAPI) (Sigma–Aldrich) for the visualization of all nuclei. Images were captured under fluorescence microscopy (Olympus, Japan) and analyzed using the ImageJ software program (NIH). The numbers of immunopositive cells were counted in four or five random areas. Approximately 1000 DAPI-stained cells were used to calculate the proportion of immunopositive cells.

2.5. Reverse transcription polymerase chain reaction (RT-PCR)

Total RNA was extracted from undifferentiated hESCs using an RNeasy mini kit (Qiagen) according to the manufacturer's protocol. Total RNA was subjected to cDNA synthesis using the SuperScript III Reverse Transcriptase (Invitrogen). A semi-quantitative RT-PCR was carried out using the primers listed in Supplementary Table S1.

2.6. Immunoblotting

Protein extracts were prepared on ice in RIPA buffer (Sigma–Aldrich) supplemented with a protease inhibitor cocktail (PIERCE). The protein concentration was determined using a BCA protein assay kit (PIERCE). The protein extracts were resolved on a 5–20% Tris-glycine acrylamide gel (Cosmobio, Japan) and transferred to a PVDF membrane (Bio-Rad) for immunoblotting. To detect PS1 proteins, a polyclonal antibody against the N-terminal region of the PS1 protein (Santa Cruz Biotechnology), horseradish peroxidase (HRP)-conjugated anti-rabbit IgG antibody (Cell Signaling Technology), an ECL Plus Western Blotting Detection System (GE Healthcare), and a LAS-3000 Bioimaging Analyzer System (Fuji Film, Japan) were used. β-actin, which was used as a loading control, was detected by a monoclonal antibody against β-actin (Applied Biological Materials) and HRP-conjugated anti-mouse IgG antibody (Cell Signaling Technology).

2.7. The enzyme-linked immunosorbent assays (ELISAs) for the measurement of PS1 protein and amyloid beta expression levels

For the measurement of PS1 protein, PS1 was measured in the protein extracted from cells using a Human Presenilin-1 N-Term DuoSet ELISA Development kit (R&D Systems) according to the manufacturer's protocol. The amounts of Aβ40, 42 and 43 in the culture media were measured using Human Amyloid β Assay Kits (IBL, Japan) according to the manufacturer's protocol. N-[N-(3,5-difluorophenacetyl-L-alanyl)]-S-phenyglycine t-butyl ester (DAPT) (Calbiochem) was used to inhibit γ-secretase in the hESC-derived neurons. The IC50 values were calculated using a MasterPlex ReaderFit system (Hitachi Solutions, Japan).

2.8. Patch-clamp recordings

An electrophysiological analysis was performed using hESC-derived neurons which were cultured for more than 2 weeks in a maturation culture stage. An HEKA EPC10 amplifier (HEKA Instruments Inc) was used for recording data in a whole cell patch

clamp configuration. To measure the frequency of the spontaneous postsynaptic currents, an external solution (140 mM NaCl, 5 mM KCl, 10 mM HEPES, 2 mM $CaCl_2$, 1 mM $MgCl_2$, and 10 mM glucose) was adjusted to pH 7.2 with NaOH. A pipette solution (130 mM Kaspartate, 1 mM $MgCl_2$, 10 mM EGTA, 3 mM ATP-Mg, and 10 mM HEPES) was adjusted to pH 7.2 with KOH. Neurons were voltage-clamped at −60 mV or −30 mV to detect spontaneous excitatory postsynaptic currents (EPSCs) or spontaneous inhibitory post-synaptic currents (IPSCs), respectively. The inward and outward current events were recorded as sEPSCs and as sIPSCs, respectively, for 60 s.

2.9. Electron microscopy

The hESC-derived neurons on the cover slips (15 mm in diameter, *Thermanox*, Nunc) were chemically fixed with 2% glutaraldehyde in NaHCa buffer (100 mM NaCl, 30 mM HEPES, 2 mM $CaCl_2$, adjusted at pH 7.4 with NaOH). The procedures that followed were performed as described in our previous paper [22], with the exception that the post-fixed specimens were embedded in Epon812 resin (TAAB Laboratories Equipment Ltd, UK).

3. Results

3.1. The generation of PS1-overexpressing hESC lines

To establish hESCs that overexpressed wild-type or mutant PS1, we utilized the site-directing gene integration system that we developed in a previous study [19]. Using this system, an exogenous gene of interest can be inserted into the *HPRT1* locus. As described in the Materials and Methods, the PS1 expression vectors (wild-type PS1, PS1−P117L, PS1-G378E or PS1-D385A) were introduced into the defined site of the genome. The PS1 protein expression level was examined to confirm the overexpression of exogenous PS1 (Fig. 1A). The bands of the full-length PS1 were detected in all of the drug-resistant clones that we tested, while the full-length protein bands were not detected in the parent cell line KhES-1-HS. In a dominant-negative mutant PS1-D385A (PS1-D clones), N-terminal fragments of PS1 (which are generated by endoproteolysis) were not detected by immunoblotting. Because Aspartate 385 is important for endoproteolysis [23], the PS1 proteins produced from the expression vectors were not self-digested. These data indicate that the PS1 proteins were overexpressed in these clones. Furthermore an ELISA showed the overexpression of PS1 in these clones (Fig. 1B). The ELISA also indicated that the PS1 protein expression levels were almost the same among the clones that expressed wild-type or mutant PS1 genes. These data were expected because all of the clones had exogenous PS1 genes in the same site for gene integration and had an identical genetic background. On the other hand, the amount of N-terminal fragments of PS1 proteins appeared to be different (Fig. 1A), suggesting that PS1 mutations might affect the efficiency of PS1 endoproteolysis.

An RT-PCR showed that PS1-overexpressing cells maintained the expression of the pluripotent-related genes and endogenous PS1, suggesting that PS1 overexpression did not affect the expression control of these pluripotent marker genes or the endogenous PS1 gene (Fig. 1C). Next, we examined the expression of undifferentiated cell markers by immunocytochemistry (Fig. 1D). All of the colonies expressed pluripotent markers, suggesting that PS1 overexpression did not affect the undifferentiated cell status. We also examined karyotyping. Although one clone (PS1−B2) had an abnormal karyotype, the other clones had normal karyotypes (Supplementary Fig. S1). Taken together, these data indicated that PS1 overexpression did not affect chromosome stability and that the overexpression of PS1 did not affect undifferentiated status of hESCs.

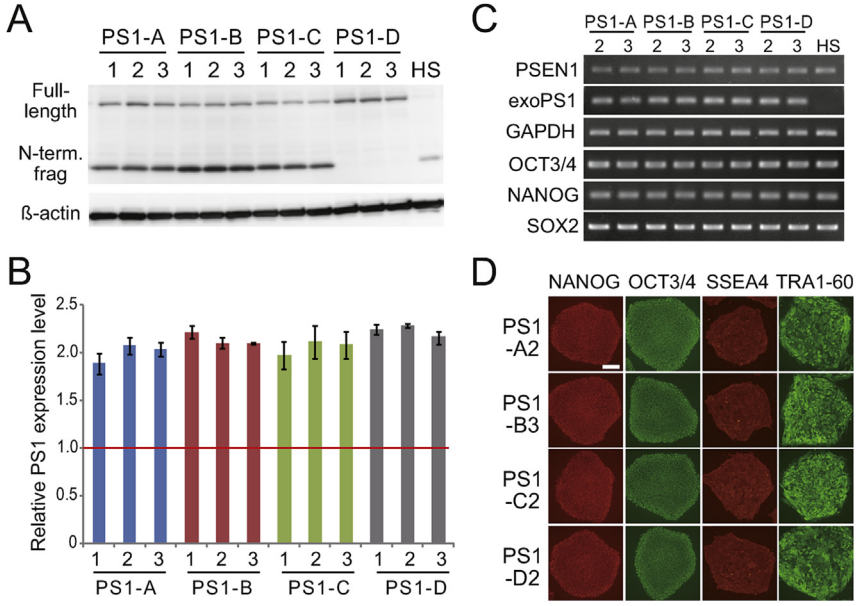

Fig. 1. The undifferentiated status of PS1-overexpressing hESCs. (A) An immunoblot analysis of PS1 overexpression in undifferentiated hESCs. An antibody against N-terminal PS1 fragment was used to detect PS1 proteins. β-actin was used as an internal control. PS1-A, -B, -C, and -D indicate wild-type, P117L, G378E, and D385A PS1-overexpressing cells, respectively. The numbers indicate the clone identification number. HS, the parental hESC line. (B) The PS1 protein expression levels were measured using ELISA. The PS1 expression levels in the parental hESCs were defined as 1.0. The mean ± SEM (n = 3). There were no statistically significant differences in the expression levels of the PS1-overexpressing clones. (C) An RT-PCR of the PS1 gene and pluripotent-related genes. The primers are listed in Supplementary Table S1. PSEN1, endogenous PS1, exoPS1, and exogenous PS1 expression on the *HPRT1* locus. NANOG, OCT3/4 and SOX2 were examined as markers of pluripotency. GAPDH was used as an internal control gene. (D) Immunostaining with undifferentiated markers. NANOG, OCT3/4, SSEA4 and TRA1-60 were used as undifferentiated markers of hESCs. Scale bar: 200 μm.

3.2. The neural differentiation of the PS1-overexpressing hESC lines

Single clones from wild-type or mutant PS1-overexpressing clones were used for further studies because there were no significant variations in the PS1 protein expression levels among any of the mutant-PS1 clones and because all of clones had an identical genetic background. First, we examined the neural differentiation ability of the PS1-overexpressing hESC lines. Neural markers, NeuN and βIII-tubulin were used to detect neurons derived from hESCs (Fig. 2A). The morphology of PS1-overexpressing neurons did not differ from the parental hESC-derived neurons. All of the cell lines showed a similar degree of neural differentiation efficiency, regardless of whether the hESC cells overexpressed the PS1 protein or not (Fig. 2B). The overexpression of PS1 protein was confirmed in differentiated neurons (Fig. 2C). Although the amount of full-length PS1 was decreased in comparison to undifferentiated cells, the N-terminal fragments of PS1 were clearly detected as thicker bands than in the parental hESC, HS. Electron microscopy demonstrated that synapses still formed as usual among these mutant PS1-expressing neurons (Fig. 2D). Collectively, these data indicate that the overexpression of PS1 does not affect the ability of hESCs to differentiate into neurons.

3.3. Increases in Aβ42 and Aβ43 secretion from mutant PS1-expressing neurons

Increased Aβ42 is a major characteristic of AD phenotypes. We measured the Aβ42/Aβ40 ratio in the culture medium of the hESC-derived neurons by an ELISA (Fig. 3A). The Aβ42 ratio was clearly increased in mutant PS1-expressing neurons (PS1−B3 and PS1−C2), while the wild-type and the dominant-negative PS1-expressing neurons (PS1-A2 and PS1-D2) did not differ from the parent cells. We also found that the amount of Aβ43, one of the Aβ species, was clearly increased in PS1−C2 (G378E mutation) alone. These data are consistent with a previous report which indicated that the amount of Aβ43 differed among PS1 mutant types [24].

Next, we examined the reactivity of our AD models to a γ-secretase inhibitor (DAPT). First, to accurately measure the IC50 values of DAPT in our AD models, we determined the culture period of the hESC-derived neurons. A three-week culture was not sufficient to perform an accurate IC50 measurement, but there was no significant difference between the 4- and 5-week cultures, which suggested that more than 4 weeks of culture was required to accurately determine the IC50 values of DAPT (Fig. 3C). We then calculated the IC50 values of DAPT for wild-type and mutant PS1-expressing neurons using culture media that was cultivated for 4 weeks. There were no statistically significant differences among them (Fig. 3D), indicating that the mutant PS1-overexpressing neurons show normal responsiveness to γ-secretase inhibitors. In fact, our AD models responded to other known γ-secretase inhibitors, such as BMS-708163 (Avagacestat), LY450139 (Semagacestat) and MK-0752 (data not shown). These data suggest the potential use of our AD models as tools for the AD drug screening system.

3.4. The alteration of the excitatory synapse activity of mutant PS1-expressing neurons

We next examined the electrophysiological features of our AD models to evaluate the functional alteration in neurons. Patch clamp analyses showed that there were no statistically significant differences in the action potential amplitude and frequency of PS1-expressing neurons (Fig. 4A and 4B). However, we found that

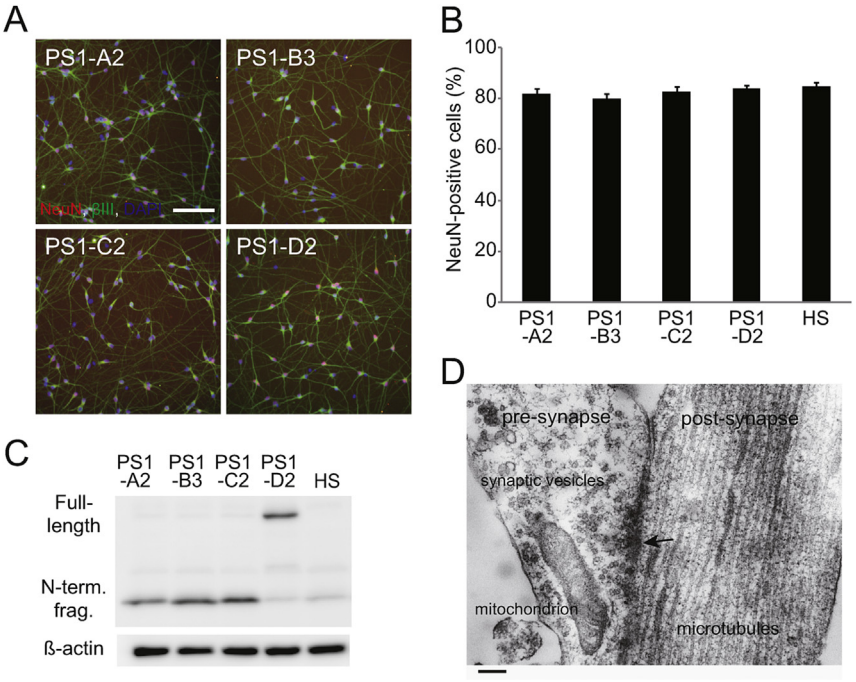

Fig. 2. The neural differentiation of PS1-overexpressing hESCs. (A) The immunostaining of neurons derived from PS1-overexpressing hESCs. NeuN (red) and βIII-tubulin (βIII, green) were used as neuronal markers. DAPI (blue) was used to visualize nuclei. Scale bar: 100 μm. (B) The ratio of NeuN-positive cells in differentiated cells. The ratio was calculated using approximately 1000 DAPI-stained cells. The mean ± SEM (n = 3). There were no statistically significant differences among the parental hESCs (HS) and the PS1-overexpressing hESCs (PS1-A2, PS1−B3, and PS1−C2). (C) An immunoblot analysis of PS1 overexpression in differentiated neurons derived from hESCs. An antibody against N-terminal PS1 fragment was used to detect PS1 proteins. β-actin was used as an internal control. (D) A transmission electron micrograph of PS1−C2-derived neurons. A characteristic postsynaptic density (arrow) was clearly observed at the site of contact between the two processes, including one on the left displaying a cluster of synaptic vesicles and a mitochondrion, which is typical of the presynapses, and another on the right displaying abundant microtubules and a few elongated elements of smooth ER, which is typical of postsynaptic dendrites or axons. Scale: 200 nm.

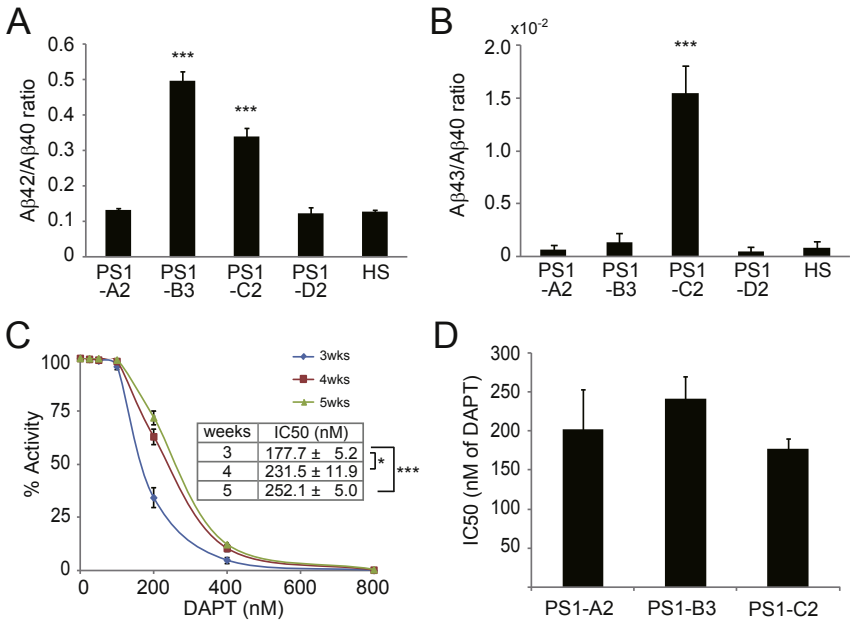

Fig. 3. The analysis of Aβ peptides secreted by PS-overexpressing neurons. (A, B) The ratios of Aβ42/Aβ40 (A) and Aβ43/Aβ40 (B). The amounts of Aβ40, 42 and 43 in the culture media were measured by an ELISA. The mean ± SEM (n = 5). ***p < 0.001 in comparison to PS1-A2 (two-tailed Student's *t*-test). (C) The responsiveness of hESC-derived neurons to a γ-secretase inhibitor (DAPT). After plating the differentiated cells for 3, 4, and 5 weeks of neural maturation with DAPT (0, 25, 50, 100, 200, 400 and 800 nM), the culture media were harvested and the Aβ40 concentration was measured. ***p < 0.001 and *p < 0.05 (two-tailed Student's *t*-test). There were no statistically significant differences between the 4- and 5-week neurons. The mean ± SEM (n = 3). (D) The IC50 values of DAPT for PS1-overexpressing neurons. The culture media were harvested at 4 weeks after plating for neural maturation and the IC50 values of DAPT were calculated. There were no statistically significant differences between the wild-type and mutant PS1-overexpressing neurons. The mean ± SEM (n = 3).

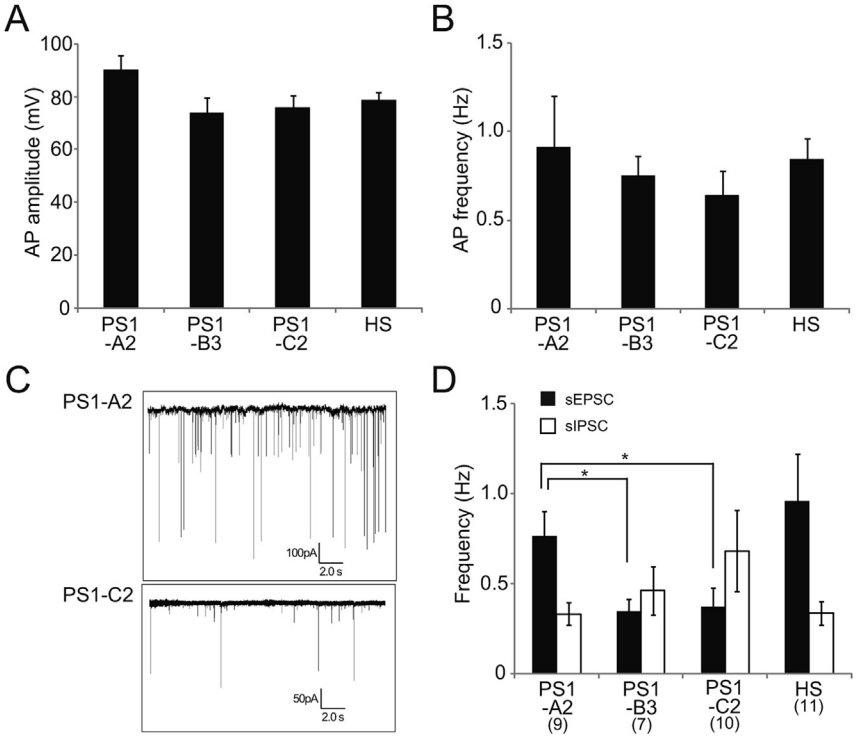

Fig. 4. The electrophysiological features of mutant PS1-expressing neurons. (A, B) The action potential (AP) amplitude (A) and AP frequency (B) of the PS1-overexpressing neurons. They did not differ from PS1-A2 to a statistically significant extent (two-tailed Student's *t*-test). The mean ± SEM (n = 9; n = 10 for PS1–C2). (C) Representative sEPSC data from wild-type and mutant PS1-expressing neurons (PS1-A2 and PS1–C2). (D) The frequencies of sEPSCs and sIPSCs. *p < 0.05 in comparison to PS1-A2 (two-tailed Student's *t*-test). The mean ± SEM (number).

frequency of spontaneous excitatory postsynaptic current (sEPSC) was significantly reduced in the mutant PS1-expressing neurons

(PS1−B3 and PS1−C2) in comparison to wild-type PS1-expressing neurons (PS1-A2), while the frequency of spontaneous inhibitory postsynaptic current (sIPSC) was not altered (Fig. 4C and D). These data suggested that PS1-overexpressing neurons could show synaptic alterations and that they may be useful as a cellular model of AD.

4. Discussion

In the present study, we established cellular models of AD which overexpressed mutant PS1 genes. We recently reported that the overexpression of mutant SOD1 was useful for showing ALS phenotypes [25]. These ALS models were established by a random integration method using mutant SOD1 cDNAs; hence the genetic expression of exogenous SOD1 was suppressed in some clones during neural differentiation [25]. However, this study showed that the expression of exogenous PS1 in the AD models was never silenced; although a slight reduction was observed in the hESC-derived neurons - perhaps because of the property of the promoter used in the present study.

In addition, the expression levels of exogenous PS1 were almost the same among different clones with the same mutation. These results suggest that the use of a site-specific gene integration system enables a strict comparative analysis among the mutations in a gene of interest. We found that the ratio of Aβ42/Aβ40 or Aβ43/Aβ40, and that the amount of PS1 fragment after self-proteolysis differed in 2 different PS1 mutations (P117L and. G378E), suggesting that these differences might reflect the properties of PS1 mutation. In addition, we recently reported that the ALS models generated by our gene integration method showed differential drug responses depending on the SOD1 mutations [20]. Thus, it is of interest whether different AD models show similarly mutation-dependent drug responses.

Several papers have reported the usefulness of AD patient-specific iPS cells in AD research (reviewed in Ref. [16]). However, these models did not show electrophysiological abnormalities. In contrast, our AD models showed synaptic dysfunction, indicating that our AD model has an advantage in the study of synaptic abnormalities using healthy and diseased cells with an identical genetic background. Future studies should address the cause of the synaptic abnormality in our AD models. Also, like the reduction of Aβ production, the restoration of synaptic dysfunction in our AD models might be a useful indicator in discovering drugs to treat AD. In conclusion, our AD models which overexpress mutant PS1 are useful tools for AD research as well as AD patient-iPSC-derived models.

Conflict of interest

There are no conflicts of interest to declare except N. Nakatsuji who holds stock in ReproCELL Inc and M. Honda who now is an employee of ReproCELL Inc.

Acknowledgments

This work was supported in part by grants from the New Energy and Industrial Technology Development Organization (P05010 to N.N.), and iCeMS (exploratory grant for junior investigators to K.A). The iCeMS is supported by World Premier International Research Center Initiative (WPI), MEXT, Japan.

Appendix A. Supplementary data

Supplementary data related to this article can be found at http://dx.doi.org/10.1016/j.bbrc.2015.12.025.

References

[1] T. Iwatsubo, A. Odaka, N. Suzuki, H. Mizusawa, N. Nukina, Y. Ihara, Visualization of Aβ42(43) and Aβ40 in senile plaques with end-specific Aβ monoclonals: evidence that an initially deposited species is Aβ42(43), Neuron 13 (1994) 45–53.
[2] C. Haass, D.J. Selkoe, Soluble protein oligomers in neurodegeneration: lessons from the Alzheimer's amyloid beta-peptide, Nat. Rev. Mol. Cell Biol. 8 (2007) 101–112.
[3] Y.-M. Kuo, M.R. Emmerling, C. Vigo-Pelfrey, T.C. Kasunic, J.B. Kirkpatrick, G.H. Murdoch, M.J. Ball, A.E. Roher, Water-soluble A(N-40, N-42) oligomers in normal and Alzheimer disease brains, J. Biol. Chem. 271 (1996) 4077–4081.
[4] W.G. Honer, Pathology of presynaptic proteins in Alzheimer's disease: more than simple loss of terminals, Neurobiol. Aging 24 (2003) 1047–1062.
[5] G.M. Shankar, S. Li, T.H. Mehta, A. Garcia-Munoz, N.E. Shepardson, I. Smith, F.M. Brett, M.A. Farrell, M.J. Rowan, C.A. Lemere, C.M. Regan, D.M. Walsh, B.L. Sabatini, D.J. Selkoe, Amyloid-β protein dimers isolated directly from Alzheimer's brains impair synaptic plasticity and memory, Nat. Med. 14 (2008) 837–842.
[6] F. Deák, Neuronal vesicular trafficking and release in age-related cognitive impairment, J. Gerontol. Ser. A Biol. Sci. Med. Sci. 69 (2014) 1325–1330.
[7] L.M. Bekris, C.E. Yu, T.D. Bird, D.W. Tsuang, Genetics of Alzheimer disease, J. Geriatr. Psychiatry Neurol. 23 (2010) 213–227.
[8] I. Piaceri, B. Nacmias, S. Sorbi, Genetics of familial and sporadic Alzheimer's disease, Front. Biosci. 5 (2013) 167–177.
[9] C. Haass, D.J. Selkoe, Cellular processing of β-amyloid precursor protein and the genesis of amyloid β-peptide, Cell 75 (1993) 1039–1042.
[10] G. Thinakaran, E.H. Koo, Amyloid precursor protein trafficking, processing, and function, J. Biol. Chem. 283 (2008) 29615–29619.
[11] K. Duff, C. Eckman, C. Zehr, X. Yu, C.-M. Prada, J. Perez-tur, M. Hutton, L. Buee, Y. Harigaya, D. Yager, D. Morgan, M.N. Gordon, L. Holcomb, L. Refolo, B. Zenk, J. Hardy, S. Younkin, Increased amyloid-β42(43) in brains of mice expressing mutant Presenilin 1, Nature 383 (1996) 710–713.
[12] G. Elder, M. Gama Sosa, R. De Gasperi, D. Dickstein, P. Hof, Presenilin transgenic mice as models of Alzheimer's disease, Brain Struct. Funct. 214 (2010) 127–143.
[13] D. Laustriat, J. Gide, M. Peschanski, Human pluripotent stem cells in drug discovery and predictive toxicology, Biochem. Soc. Trans. 38 (2010) 1051–1057.
[14] I. Gunaseeli, M. Doss, C. Antzelevitch, J. Hescheler, A. Sachinidis, Induced pluripotent stem cells as a model for accelerated patient-and disease-specific drug discovery, Curr. Med. Chem. 17 (2010) 759.
[15] H. Inoue, S. Yamanaka, The use of induced pluripotent stem cells in drug development, Clin. Pharmacol. Ther. 89 (2011) 655–661.
[16] A.A. Sproul, Being human: the role of pluripotent stem cells in regenerative medicine and humanizing Alzheimer's disease models, Mol. Asp. Med. 43–44 (2015) 54–65.
[17] M. Li, K. Suzuki, N.Y. Kim, G.-H. Liu, J.C. Izpisua Belmonte, A cut above the rest: targeted genome editing technologies in human pluripotent stem cells, J. Biol. Chem. 289 (2014) 4594–4599.
[18] J.A. Doudna, E. Charpentier, The new frontier of genome engineering with CRISPR-Cas9, Science 346 (2014).
[19] K. Sakurai, M. Shimoji, C.G. Tahimic, K. Aiba, E. Kawase, K. Hasegawa, Y. Amagai, H. Suemori, N. Nakatsuji, Efficient integration of transgenes into a defined locus in human embryonic stem cells, Nucleic Acids Res. 38 (2010) e96.
[20] T. Isobe, N. Tooi, N. Nakatsuji, K. Aiba, Amyotrophic lateral sclerosis models derived from human embryonic stem cells with different superoxide dismutase 1 mutations exhibit differential drug responses, Stem Cell Res. 15 (2015) 459–468.
[21] H. Suemori, K. Yasuchika, K. Hasegawa, T. Fujioka, N. Tsuneyoshi, N. Nakatsuji, Efficient establishment of human embryonic stem cell lines and long-term maintenance with stable karyotype by enzymatic bulk passage, Biochem. Biophys. Res. Commun. 345 (2006) 926–932.
[22] I. Minami, K. Yamada, T.G. Otsuji, T. Yamamoto, Y. Shen, S. Otsuka, S. Kadota, N. Morone, M. Barve, Y. Asai, T. Tenkova-Heuser, J.E. Heuser, M. Uesugi, K. Aiba, N. Nakatsuji, A small molecule that promotes cardiac differentiation of human pluripotent stem cells under defined, cytokine- and xeno-free conditions, Cell Rep. 2 (2012) 1448–1460.
[23] M.S. Wolfe, W. Xia, B.L. Ostaszewski, T.S. Diehl, W.T. Kimberly, D.J. Selkoe, Two transmembrane aspartates in presenilin-1 required for presenilin endoproteolysis and gamma-secretase activity, Nature 398 (1999) 513–517.
[24] T. Saito, T. Suemoto, N. Brouwers, K. Sleegers, S. Funamoto, N. Mihira, Y. Matsuba, K. Yamada, P. Nilsson, J. Takano, M. Nishimura, N. Iwata, C. Van Broeckhoven, Y. Ihara, T.C. Saido, Potent amyloidogenicity and pathogenicity of Abeta43, Nat. Neurosci. 14 (2011) 1023–1032.
[25] T. Wada, S.K. Goparaju, N. Tooi, H. Inoue, R. Takahashi, N. Nakatsuji, K. Aiba, Amyotrophic lateral sclerosis model derived from human embryonic stem cells overexpressing mutant superoxide dismutase 1, Stem Cells Transl. Med. 1 (2012) 396–402.